morphogenesis of the diatom cell wall. A completely different type of protein, a member of the papain family of proteolytic enzymes, was recently shown to be associated with silica spicules of a marine sponge (*23*). This protein catalyzes in vitro hydrolysis of silicon ethoxides (*24*) and thus may be involved in releasing silicic acid from a putative precursor molecule in vivo. In contrast, silaffins are ideally adapted to promote silicic acid polycondensation and precipitation of biogenic silica. First, as pointed out by Iler (*19*), possible candidates for flocculating agents involved in silica precipitation are cationic polymers and hydrogen-bonding polymers. Exactly these structural elements are present in silaffins, which are polycationic molecules containing a high proportion of hydroxyamino acids (predominantly serine) and are thus ideally suited for ionic and hydrogen-bonding interactions with the surface of silica particles. Second, silaffins are covalently modified by the oligo-*N*-methyl-propylamine unit that chemically resembles the polyamine structures found to catalyze silicic acid polymerization (*25*) and to promote silica flocculation (*26*). The modifications strongly increase the cationic charge of silaffins and were shown to be essential for silica formation at acidic pH values. Diatom SDVs have been shown to be acidic compartments (*18*), and therefore the polyamine structure is indispensable for silaffins to exert silica precipitation activity at the pH conditions within the SDV lumen. To our knowledge, the oligo-*N*-methyl-propylamine modification has not yet been found in any other biological system. Further analysis of the role of silaffins in nanofabrication of diatom cell walls might offer biomimetic approaches for the synthesis of siloxane-based materials.

References and Notes

1. S. Mann, *Nature* **365**, 499 (1993).
2. S. Oliver, A. Kupermann, N. Coombs, A. Lough, G. A. Ozin, *Nature* **378**, 47 (1995).
3. S. Mann and G. Ozin, *Nature* **382**, 313 (1996).
4. S. Mann, J. Webb, R. J. P. Williams, Eds., *Biomineralization: Chemical and Biochemical Perspectives* (VCH, Weinheim, Germany, 1989).
5. J. Pickett-Heaps, A. M. M. Schmid, L. A. Edgar, in *Progress in Phycological Research*, F. E. Round and D. J. Chapman, Eds. (Biopress, Bristol, UK, 1990), vol. 7, pp. 1–169.
6. B. E. Volcani, in *Silicon and Siliceous Structures in Biological Systems*, T. L. Simpson and B. E. Volcani, Eds. (Springer, New York, 1981), pp. 157–200.
7. R. Gordon and R. W. Drum, *Int. Rev. Cytol.* **150**, 243 (1994).
8. T. Nakajima and B. E. Volcani, *Science* **164**, 1400 (1969).
9. R. Hecky, K. Mopper, P. Kilham, T. Degens, *Mar. Biol.* **19**, 323 (1973).
10. D. Swift and A. Wheeler, *J. Phycol.* **28**, 202 (1992).
11. N. Kröger, C. Bergsdorf, M. Sumper, *EMBO J.* **13**, 4676 (1994).
12. N. Kröger, G. Lehmann, R. Rachel, M. Sumper, *Eur. J. Biochem.* **250**, 99 (1997).
13. H. Schägger and G. von Jagow, *Anal. Biochem.* **166**, 368 (1987).
14. Silica precipitation assay. A solution of orthosilicic acid was freshly prepared by dissolving tetramethylorthosilicate ester in 1 mM HCl to a final concentration of 1 M. Proteins to be tested for silica precipitation activity were dissolved in 100 mM sodium phosphate–citrate (buffered to the appropriate pH) to a final volume of 10 μl. Subsequently, 1 μl of the 1 M orthosilicic acid solution was added and samples were incubated for 5 min at ambient temperature. Samples were centrifuged for 5 min at 14000*g* and pellets were washed three times with H_2O to remove free silicic acid and phosphate. Washed pellets were resuspended in 10 μl of 1 M NaOH and silica was dissolved by incubation at 95°C for 30 min. Silicium concentrations were determined in these solutions by the β-silicomolybdate method (*19*).
15. Purification of silaffin-1A. HF extract from *C. fusiformis* cell walls was prepared as described (*12*) and fractionated on a size-exclusion column (Superdex-Peptide HR-10/30, Amersham Pharmacia Biotech). Chromatography was performed in buffer A [250 mM NaCl, 20 mM tris-HCl (pH 7.5)] at a flow rate of 250 μl/min. Eluting material was recorded at 226 nm and fractions were analyzed by Tricine–SDS-PAGE (*13*) and Coomassie blue staining. Fractions containing pure silaffin-1A were pooled, dialyzed against H_2O, lyophylized, and dissolved in H_2O to a final protein concentration of 10 to 30 μmol/ml.
16. N. Kröger, R. Deutzmann, M. Sumper, data not shown.
17. N. Kröger, C. Bergsdorf, M. Sumper, *Eur. J. Biochem.* **239**, 259 (1996).
18. E. G. Vrieling, W. W. C. Gieskes, T. P. M. Beelen, *J. Phycol.* **35**, 548 (1999).
19. R. K. Iler, *The Chemistry of Silica* (Wiley, New York, 1979).
20. M. L. Chiappino and B. E. Volcani, *Protoplasma* **93**, 205 (1977).
21. M. A. Borowitzka and B. E. Volcani, *J. Phycol.* **14**, 10 (1978).
22. A. M. M. Schmid and D. Schulz, *Protoplasma* **100**, 267 (1979).
23. K. Shimizu, J. Cha, G. Stucky, D. E. Morse, *Proc. Natl. Acad. Sci. U.S.A.* **95**, 6234 (1998).
24. J. Cha *et al.*, *Proc. Natl. Acad. Sci. U.S.A.* **96**, 361 (1999).
25. T. Mitzutani, H. Nagase, N. Fujiwara, H. Ogoshi, *Bull. Chem. Soc. Jpn.* **71**, 2017 (1998).
26. G. M. Lindquist and R. Stratton, *J. Colloid Interface Sci.* **55**, 45 (1976).
27. Protein concentration was determined by the bicinchoninic acid assay as described [P. K. Smith *et al.*, *Anal. Biochem.* **150**, 76 (1985)].
28. Peptide concentration was determined after acid hydrolysis by HPLC analysis of the PTC amino acid derivatives.

29. We thank G. Lehmann and E. Hochmuth for technical assistance; T. Maurer and H. R. Kalbitzer for NMR analysis; and F. Siedler and H. Sarioglou for MS/MS analysis. We are indebted to G. Wanner for field-emission SEM analysis and R. Wetherbee for help with TEM analysis. We greatfully acknowledge W. Tanner for critically reading the manuscript. This work was supported by the Deutsche Forschungsgemeinschaft (SFB 521).

21 July 1999; accepted 30 September 1999

A Possible 20th-Century Slowdown of Southern Ocean Deep Water Formation

Wallace S. Broecker,[1] Stewart Sutherland,[1] Tsung-Hung Peng[2]

Chlorofluorocarbon-11 inventories for the deep Southern Ocean appear to confirm physical oceanographic and geochemical studies in the Southern Ocean, which suggest that no more than 5 × 10^6 cubic meters per second of ventilated deep water is currently being produced. This result conflicts with conclusions based on the distributions of the carbon-14/carbon ratio and a quasi-conservative property, PO_4^*, in the deep sea, which seem to require an average of about 15 × 10^6 cubic meters per second of Southern Ocean deep ventilation over about the past 800 years. A major reduction in Southern Ocean deep water production during the 20th century (from high rates during the Little Ice Age) may explain this apparent discordance. If this is true, a seesawing of deep water production between the northern Atlantic and Southern oceans may lie at the heart of the 1500-year ice-rafting cycle.

Circulation changes in the upper ocean have been shown to be an integral part of El Niño cycles, but there has been relatively little discussion concerning the possibility that circulation changes in the deep sea have occurred during the course of the present century. The last well-documented major change in thermohaline circulation occurred in association with the Younger Dryas cold event that ended ~11,500 calendar years ago (*1*). Only at the time of the so-called 8000-years-ago cooling event is there a suggestion of a weakening in the strength of the Atlantic's large-scale circulation during the present interglacial period (*2*). Rather, circulation is often thought of in terms of a smoothly operating Holocene conveyor (*3*). Now, tantalizing evidence suggests that the current rate of deep water formation in the Southern Ocean may be several times smaller than its average over the course of the last ocean mixing cycle (that is, ~800 years).

There is an apparent inconsistency between long-term ventilation rates based on the global distributions of PO_4^* and ^{14}C and those based on observations of the Weddell Sea over the past two decades (*4*). The distribution of PO_4^* [PO_4^*

[1]Lamont-Doherty Earth Observatory of Columbia University, Palisades, NY 10964, USA. [2]Ocean Chemistry Division, Atlantic Oceanographic and Meteorological Laboratory, National Oceanic and Atmospheric Administration, Miami, FL 33149–1026, USA.

$= PO_4 + (O_2/175) - 1.95$ µmol/kg] shows that the entire deep Pacific and Indian oceans are filled with a nearly uniform mixture of water with $PO_4^* = 1.38 \pm 0.05$ µmol/kg, intermediate between $PO_4^* = 0.73$ µmol/kg for deep water formed in the northern Atlantic and $PO_4^* = 1.95$ µmol/kg for recently ventilated dense water spilling off the margin of the Antarctic continent into the abyss of the Weddell and Ross seas. Because these northern and southern source waters are completely mixed during their passage around Antarctica, we conclude that nearly equal amounts of deep water originate in the northern Atlantic and around the perimeter of the Antarctic continent. Furthermore, in order to satisfy the deep sea's ^{14}C budget over the last ventilation (mixing) cycle, each of these sources must, on the average, have supplied ~15 sverdrups [1 sverdrup = 10^6 m^3/s] of ventilated water to the deep sea (*4, 5*). This conclusion has been verified by a box-model simulation (*5*). Yet, studies carried out in the Weddell Sea show that no more than 4 sverdrups of ventilated deep water are generated in this source region (*4*). This mismatch between observations reflecting the long- and short-term operations might result from temporal variability in the strength of the Southern Ocean source or from deep water being produced in sizable quantities at other locations around the perimeter of Antarctica. The resolution of this seeming inconsistency may lie in the deep sea chlorofluorocarbon (CFC) inventories (*6*).

The completion of the World Ocean Circulation Experiment (WOCE) program in the Southern Ocean has made adequate information available to permit the compilation of a reliable inventory of deep Southern Ocean CFCs. Only over the past few decades has newly ventilated deep water carried these tracers. Newly produced deep water in the Southern Ocean is saturated to ~70% with CFC-11 (Fig. 1). On the available time scale (a few decades), little of this tracer is returned to the surface. Furthermore, because of the high measurement sensitivity, little of this tracer has escaped detection as the result of dilution during its spread away from the source regions. On the basis of an integration of Southern Ocean CFC-11 (*7*), we conclude that, over the past several decades, ventilated bottom water (*8*) has formed at an average rate of 4 sverdrups. In contrast, CFC-11 inventories for the northern Atlantic yield a production rate of deep water broadly consistent with that required to balance the Atlantic's natural ^{14}C budget (*9*). Thus, the CFC inventories seem to rule out the hypothesis that other as yet unmapped source regions around the perimeter of the Antarctic continent are currently heavy contributors to deep water production. This finding suggests that ventilation of the deep Southern Ocean is episodic rather than steady.

Processes operating along the margins of the Weddell and Ross seas may be incapable of supplying much more than 4 sverdrups of ventilated deep water. If so, then polynyas or open ocean convective cells must be responsible for the much higher past production of ventilated deep water. If such events have supplied an average of ~10 sverdrups of ventilated deep water at times in the past, their frequency must at that time have been far greater than during the past 25 years.

Although a range of scenarios could be envisioned to account for these observations, here we explore one that calls on much stronger Southern Ocean deep water formation during the Little Ice Age (~1350 to 1880 A.D.), a period of relatively cold climate in the region around the northern Atlantic that came after the so-called Medieval Warm Period.

Little is known about conditions outside of Europe during the early and middle phases of the Little Ice Age, but a much better global picture of conditions during its terminal phase is available (Fig. 2). Mountain glaciers in the Swiss Alps, the southern Andes, and the New Zealand Alps were far more extensive in the mid-1800s than they are today (*10*) or at any other time during the Holocene. Mountain snow lines descended ~100 m below their current positions (compared to ~350 m below their current positions during the Younger Dryas and 950 m below their current positions during the peak of the last glacial period). The Little Ice Age cold phase in mountainous areas came to an end during the latter part of the 19th century. By the beginning of the 20th century, mountain glaciers in temperate and tropical regions were in full retreat. This retreat has continued to the present. Further, as summarized in Fig. 1, the extensive sea ice coverage around Iceland during the 17th, 18th, and 19th centuries diminished rapidly during the early part of the 20th century.

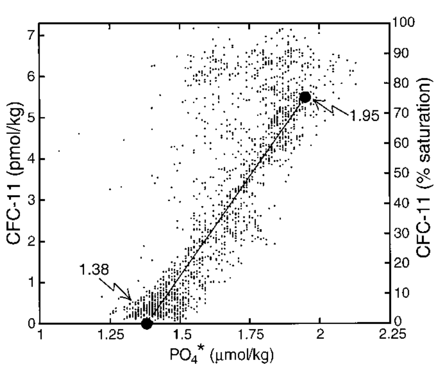

Fig. 1. CFC-11 concentration as a function of PO_4^* for waters south of 40°S from depths less than 500 m and with temperatures less than 3°C. Many of the points scatter around a mixing line joining the compositions of CFC-11 free water with a PO_4^* value of 1.38 µmol/kg (characteristic of upwelling circumpolar deep water) and water with a PO_4^* value of 1.95 µmol/kg (characteristic of newly forming deep water). Newly forming deep water is ~75% saturated with CFC-11.

During the Last Glacial Maximum (*11*) and the Younger Dryas (*12*), the pattern of the ocean's thermohaline circulation differed from today's, and it is tempting to postulate that it was different during the Little Ice Age as well. However, because the recent cold snap had a muted intensity (were such a change to have occurred during the Little Ice Age), it was likely different in character. In constructing a scenario in which the Southern Ocean ventilation was, on the average, much stronger in the past than it is currently, decisions regarding the timing of these changes must be made. If the Little Ice Age began during the 13th century (*10, 13*), then most of the last cycle of oceanic ventilation (*14*) occurred under Little Ice Age conditions, and the contribution made to the existing pattern of deep sea properties by ventilation during the preceding Medieval Warm Period can, perhaps, be disregarded. If so, then the critical issue is to define when the demise of Southern Ocean ventilation occurred. The post–Little Ice Age warming occurred in two major steps: one between 1880 and 1945 and the other from 1975 to the present (*15*). Because the ocean observations span the second of these steps, it is less likely that a change occurred during this interval. Hence, if a single transition time were to be chosen, then, most likely, it would lie in the interval from 1880 to 1945. Of course, it is possible that the transition occurred gradually over the entire 20th century and is still in progress. In any case, the post–Little Ice Age period of Southern Ocean quiescence is unlikely to exceed 100 years in duration or about one-eighth of the ocean ventilation time (*14*).

The current Southern Ocean bottom water

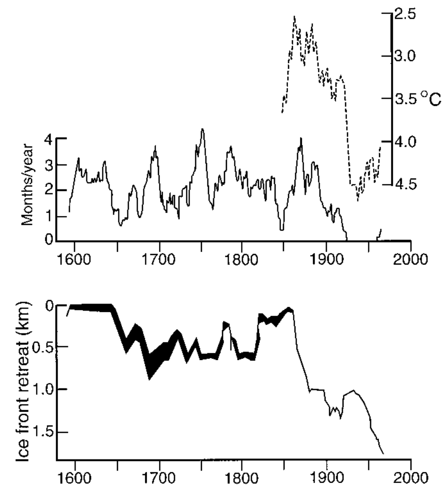

Fig. 2. Historic climate records dating to 1600 A.D. (**Top**) A record of the number of months per year that sea ice was present around Iceland (solid curve) and its relation to mean annual temperatures available since 1850 A.D. (dashed curve) (*27*). (**Bottom**) The extent of the front of the Grindelwald Glacier as reconstructed from oil paintings, drawings, prints, photographs, maps, and literature (*28*).

ventilation rate appears to be ~4 sverdrups. The constraint placed by PO_4^* and ^{14}C is that, on the average, the Southern Ocean and northern Atlantic contributions have been nearly equal and have totaled ~30 sverdrups over the course of the last ventilation cycle. Therefore, depending on the duration of the recent near shutdown, the rate during the Little Ice Age must have been correspondingly greater than 15 sverdrups. Of course, we would like to think that the production of deep water in the northern Atlantic was weaker during the Little Ice Age. However, the uncertainties in the ^{14}C-based estimate for the average ventilation rate over the past 200 years and in present-day ventilation rates (including the CFC-based estimate) are too large to lend support to such a conclusion.

During the interval of the last deglaciation, the temperature changes on the Antarctic polar cap were antiphased with respect to those on the rest of the planet (*16–18*). In particular, during the pronounced Bolling-Allerod warm interval, which brought to an end glacial conditions everywhere north of 45°S, the warming that had been underway in Antarctica during the previous 5000 years stalled. Only when the rest of the planet was plunged back into the cold Younger Dryas conditions did the warming in Antarctica resume. One explanation that has been proposed for this antiphasing is that an alternation between intense deep water formation in the northern Atlantic and in the Southern Ocean occurred (*19, 20*). Strong support for this idea comes from a reconstruction of the ^{14}C content of atmospheric and upper ocean C (*1*). This record requires a 5% rise in ^{14}C content of these reservoirs during the first two centuries of the Younger Dryas. Only a conveyor shutdown provides a reasonable explanation for this rise (*1, 19, 20*). The climatic consequence of this bipolar seesaw could be a warming of Antarctica during the periods of intense deep water formation in the Southern Ocean and, of course, a cooling of the region around the northern Atlantic (*19, 20*).

This raises the question of whether the continent of Antarctica experienced warmer conditions during the Little Ice Age, when the region around the northern Atlantic was cooler and the extent of sea ice around Iceland was greater. The preliminary results of a deconvolution of the borehole temperature record obtained at Taylor Dome, Antarctica, suggests that temperatures were 3°C warmer during the Little Ice Age than they were during the Medieval Warm Period (*21*). If this preliminary conclusion withstands further scrutiny, then the pattern of global temperature change for the Little Ice Age would appear to be consistent with that for the Younger Dryas and, therefore, with greater deep water formation in the Southern Ocean at that time. At this point, a caveat is necessary; we do not understand how the change in deep ocean ventilation generated the observed magnitude of global temperature change (*22*).

One might ask whether such a dramatic change in deep ventilation created a pattern of deep ocean properties that might contradict the assumption that the deep sea is at steady state. The answer is that there is nothing about the present-day distribution of properties that is inconsistent with steady state ventilation. The question must then be asked in another way: Where in the distribution of these properties would one look for features that might point to stronger Southern Ocean ventilation during the Little Ice Age? The most obvious place is the deep Southern Ocean. One would expect that the current dominance of northern component water would have reduced the PO_4^* for deep waters in the Southern Ocean below those for the interior of the deep Indian and Pacific oceans. Plots (Fig. 2) of PO_4^* versus dissolved O_2 (an index of the "age" of the water) show no discernible trend in PO_4^* in the deep Pacific or deep Indian oceans. Furthermore, there is only a slight indication that the PO_4^* in deep Southern Ocean water has decreased.

Using a 10-box ocean model, we have explored, in a preliminary way, the impact on the PO_4^* value for the deep Southern Ocean of a fourfold 100-year duration reduction in the rate of deep water formation in the south. As expected, the PO_4^* concentration of the deep Southern Ocean box undergoes a shift toward that for northern source water. After 100 years, the PO_4^* value for Southern Ocean deep water should have dropped by 12%. A reduction of this magnitude is not seen (Fig. 3). This may represent the shortcomings of the simple model, a flaw in our view of the data, or the failure of our hypothesis.

Our simple box model also suggests that a 100-year slowdown of Southern Ocean deep water formation would result in an increase of 14 per mil in the $^{14}C/C$ in atmospheric CO_2 (due to a backlogging in the upper ocean and atmosphere of newly produced ^{14}C atoms). Because the ^{14}C content of the atmosphere has been decreasing over the past 200 years, first as a result of the drop in ^{14}C production after the Maunder Minimum and then due to the input of ^{14}C-free CO_2 from fossil fuel production, it will take some effort to ascertain whether or not this predicted ^{14}C rise can be accommodated.

Two sources of evidence can be explored in hopes of obtaining a hint that a shift has indeed occurred. One is to contrast the results of temperature and salinity surveys made in the 1930s by the German oceanographic vessel *Meteor* to determine whether the northward penetrating wedge of colder and less salty bottom water in the western Atlantic AABW (Antarctic Bottom Water) has retreated during the past 60 years. This has yet to be done. The other is to study high-deposition-rate sediments for a ^{13}C and Cd change in benthic foraminifera shells formed during the Little Ice Age. Sediment in a core with a very high accumulation rate from near Bermuda shows a ^{13}C drop consistent with a greater extent of the AABW wedge during the Little Ice Age, but Cd measurements are at odds with this conclusion (*23*).

If the thermohaline hypothesis were to gain support, then the question will surely arise as to whether the Little Ice Age was a onetime event in the Holocene or whether it is part of a continuing cycle. Ice-rafting events in the northern Atlantic recur at ~1500-year intervals (*24, 25*). No evidence exists for a substantial

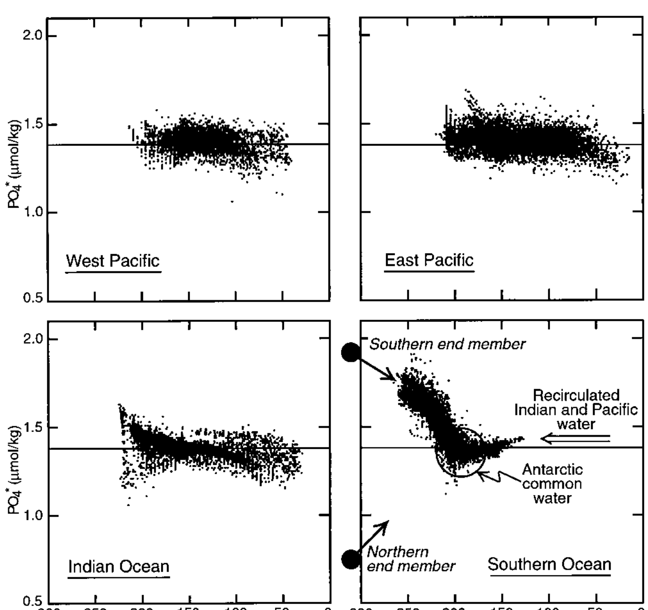

Fig. 3. PO_4^* versus O_2 for the deep waters in the Pacific, Indian, and Southern oceans. The O_2 and PO_4 measurements were made as part of the Geochemical Ocean Sections Study, South Atlantic Ventilation Experiment, and WOCE expeditions. For the Pacific and Indian oceans, all samples from greater than 1500 m northward of 40°S are included. For the Southern Ocean, all samples from greater than 1000 m depth and with dissolved silica contents greater than 90 μmol/kg are included. There is only a slight indication that Southern Ocean common water values are lower than those for the deep Indian and Pacific oceans, as would be expected if the input of high-PO_4^* southern end-member water had been greatly reduced during the 20th century.

external forcing with this time constant, but 1500 years is a reasonable time constant for an oscillation involving large-scale ocean circulation. This can be seen as follows. On the basis of a combination of atmospheric measurements and model simulations, it has been estimated that water vapor is being transported from the Atlantic Ocean to the Pacific and Indian oceans at the average rate of $0.25 \pm 0.10 \times 10^6$ m^3/s (*26*). Were this loss not compensated by salt export, the salinity of the Atlantic would increase by ~1 g/liter in 1500 years. Such an increase would have the same impact on the density of cold surface waters as a 5°C cooling would. Hence, one could envision that the export of salt required to balance its buildup in the Atlantic is cyclic rather than uniform.

One element in the debate regarding the consequences of the ongoing buildup of greenhouse gases has to do with distinguishing the contributions of natural and anthropogenic climate change. The post–Little Ice Age warming that occurred during the first half of the 20th century is comparable in magnitude to warming that occurred between 1975 and the present. During the former period, little buildup of greenhouse gases occurred. During the latter, an immense buildup has occurred. Those who call for action designed to stem the pace of the greenhouse buildup firmly believe that the warming during the latter part of the century was greenhouse driven. Those opposed to action would like to explain the entire warming as mainly natural. Thus, one of our tasks is to gain a better understanding of the Little Ice Age and its demise. If, as proposed here, changes in thermohaline are indeed involved, then a step toward this goal will have been taken.

References and Notes

1. K. A. Hughen *et al.*, *Nature* **391**, 65 (1998).
2. D. C. Barber *et al.*, *Nature* **400**, 344 (1999).
3. The conveyor refers to the large-scale circulation in the Atlantic Ocean. Warm waters in the upper 1500 m flow northward to the vicinity of Iceland. Winter cooling densifies this already salty water, permitting it to sink to the abyss. Once at depth, the water flows the length of the Atlantic and becomes entrained in the circum-Antarctic deep raceway. For details, see W. S. Broecker, *Oceanography* **4**, 79 (1991).
4. W. S. Broecker *et al.*, *J. Geophys. Res.* **103**, 15833 (1998).
5. S. Peacock, M. Visbeck, W. S. Broecker, in *Inverse Methods in Global Biogeochemical Cycles*, vol. 114 of *Geophysical Monograph Series* (American Geophysical Union, Washington, DC, in press).
6. E. Carmack, *Deep Sea Res. Oceanogr. Abstr.* **20**, 927 (1973); A. E. Gill, *Deep Sea Res. Oceanogr. Abstr.* **20**, 111 (1973); E. C. Carmack and T. D. Foster, *Deep Sea Res. Oceanogr. Abstr.* **22**, 77 (1975); T. D. Foster and J. H. Middleton, *J. Phys. Oceanogr.* **6**, 36 (1976); P. D. Killworth, *Deep Sea Res.* **24**, 427 (1977); R. L. Michel, *J. Geophys. Res.* **83**, 6192 (1978); R. F. Weiss, H. G. Ostlund, H. Craig, *Deep Sea Res. Part A* **26**, 1093 (1979); T. D. Foster and J. H. Middleton, *Deep Sea Res. Part A* **27**, 367 (1980); A. Foldvik, T. Gammelsrod, T. Torresen, in *Oceanology of the Antarctic Continental Shelf*, vol. 43 of *Antarctic Research Series*, S. S. Jacobs, Ed. (American Geophysical Union, Washington, DC, 1985), pp. 5–20; R. Bayer and P. Schlosser, *Mar. Chem.* **35**, 123 (1991); P. Schlosser, J. L. Bullister, R. Bayer, *Mar. Chem.* **35**, 97 (1991); A. L. Gordon, B. A. Huber, H. H. Hellmer, A. Ffield, *Science* **262** 95 (1993); E. Fahrbach *et al.*, *J. Mar. Res.* **53**, 515 (1995).
7. A. H. Orsi, G. C. Johnson, J. L. Bullister, *Prog. Oceanogr.* **43**, 55 (1999).
8. By ventilated deep water, we mean water that descended after contact with the atmosphere. As the PO_4^* value of Southern Ocean waters is reset mainly by the replenishment of O_2, it is important to exclude the contribution of older deep water entrained during the descent to the abyss. This is not to say that freshly ventilated waters are fully recharged with atmosphere gases. Measurements suggest that, in the Southern Ocean source regions, neither the O_2 nor the CFC content of the water reaches saturation. For both gases, the extent of saturation achieved appears to be ~70%. Orsi *et al.* (*7*) interpret the CFC-11 data to indicate 8 sverdrups of ventilation. On the basis of measurements of slope waters that had already entrained recirculated deep water, they assumed only 35% CFC-11 saturation. If the more reasonable 70% saturation value is adopted, then the flux of ventilated deep water drops to 4 sverdrups.
9. W. M. Smethie Jr. and R. A. Fine, *Deep Sea Res.*, in press.
10. J. M. Grove, *The Little Ice Age* (Methuen, New York, 1988).
11. E. A. Boyle, *Annu. Rev. Earth Planet. Sci.* **20**, 245 (1992); D. W. Lea and E. A. Boyle, *Nature* **338**, 751 (1989); J.-C. Duplessy *et al.*, *Paleoceanography* **3**, 343 (1988); D. W. Oppo and R. G. Fairbanks, *Earth Planet. Sci. Lett.* **86**, 1 (1987).
12. E. A. Boyle and L. D. Keigwin, *Nature* **330**, 35 (1987).
13. F. Gad, *The History of Greenland II*, *Earliest Times to 1700* (Hurst, London, 1970).
14. By ventilation time, we mean the time required for the production of new deep water to replace the water in the deep sea. Assuming a production rate of 30×10^6 m^3/s and that the volume of the deep sea is 60% of the total volume, this flushing time is 850 years.
15. M. E. Mann and R. S. Bradley, *Geophys. Res. Lett.* **26**, 759 (1999).
16. T. Sowers and M. Bender, *Science* **269**, 210 (1995).
17. R. B. Alley *et al.*, *Nature* **362**, 527 (1993).
18. D. A. Meese *et al.*, *Science* **266**, 1680 (1994).
19. W. S. Broecker, *Paleoceanography* **13**, 119 (1998).
20. T. F. Stocker, *Science* **282**, 61 (1998).
21. G. Clow, personal communication.
22. W. S. Broecker, *Science* **278**, 1582 (1997).
23. L. Keigwin, *Proc. Natl. Acad. Sci. U.S.A.*, in press.
24. G. Bond *et al.*, *Science* **278**, 1257 (1997).
25. R. A. Kerr, *Science* **284**, 2069 (1999).
26. F. Zaucker and W. S. Broecker, *J. Geophys. Res.* **97**, 2765 (1992).
27. P. Bergthórsson, *Joekull* **19**, 94 (1969).
28. B. Messerli, P. Messerli, C. Pfister, H. J. Zumbühl, *Arct. Alp. Res.* **10**, 247 (1978).

29. Discussions with L. Keigwin, B. Smethie, G. Clow, and G. Denton raised our interest in this subject. Financial support was provided by grant ATM 97-30546 from NSF. This is Lamont-Doherty Earth Observatory contribution number 5998.

12 July 1999; accepted 6 October 1999

Fault Slip Rates in the Modern New Madrid Seismic Zone

Karl Mueller,[1] Jocasta Champion,[1] Margaret Guccione,[2] Keith Kelson[3]

Structural and geomorphic analysis of late Holocene sediments in the Lake County region of the New Madrid seismic zone indicates that they are deformed by fault-related folding above the blind Reelfoot thrust fault. The widths of narrow kink bands exposed in trenches were used to model the Reelfoot scarp as a forelimb on a fault-bend fold; this, coupled with the age of folded sediment, yields a slip rate on the blind thrust of 6.1 ± 0.7 mm/year for the past 2300 ± 100 years. An alternative method used structural relief across the scarp and the estimated dip of the underlying blind thrust to calculate a slip rate of 4.8 ± 0.2 mm/year. Geometric relations suggest that the right lateral slip rate on the New Madrid seismic zone is 1.8 to 2.0 mm/year.

The clustered sequence of large-magnitude earthquakes that occurred within the New Madrid seismic zone (NMSZ) in 1811 and 1812 left no prominent evidence of surface fault rupture (Fig. 1A). There is, however, evidence for active uplift and surface deformation during these events across the Lake County Uplift (LCU), a compressive stepover in the mostly strike-slip NMSZ (*1–3*). An increasingly well-defined chronology of paleoearthquakes in the NMSZ has been developed through dating of liquefaction features (*4*) and syntectonic sediment derived by erosion of the Reelfoot scarp and infilled grabens (*5*). Determination of prehistoric earthquake magnitude in the NMSZ is difficult to define because (i) surface fault ruptures available for paleoseismic study have not been identified and (ii) methods used to define earthquake magnitude by paleoliquefaction features have not been readily calibrated by historic events.

We used fault-related fold theory (*6*, *7*) to model the growth of the active LCU, based on trench exposures (*5*), microseismicity (*8*), high-resolution seismic reflection profiles (*9*, *10*), and digital elevation models (Fig. 1B) (*11*). The purpose of our analysis is to determine the late Quaternary slip rate for the blind Reelfoot thrust fault by using fold geometry and structural relief. We also compared our estimated slip rates for the Reelfoot

[1]Department of Geological Sciences, University of Colorado, Boulder, CO 80309–0399, USA. [2]Department of Geology, University of Arkansas, Fayetteville, AR 72701, USA. [3]William Lettis and Associates, 1777 Botelho Drive, Suite 262, Walnut Creek, CA 94596, USA.